

present case, the ionization energy of the Hg $6s^2$ valence electrons is 1.4 eV higher than that of the Cd $5s^2$. It should further be noted that the work in the early 1960's showed² that both the decrease of E_g to zero and the high electron mobilities are associated with the metal s states of the conduction band decreasing in energy with increasing Hg content until they mix with the p states to form the valence-band maximum. We thus identify three phenomena (the breakdown of VCA, E_g going to zero, and high electron mobility) as resulting from the Hg $6s^2$ atomic levels being significantly below the Cd $5s^2$ levels.

$\text{Hg}_{1-x}\text{Cd}_x\text{Te}$ is perhaps the most promising material available for photodetection throughout the infrared, yet it has not been widely exploited. This may be because of difficulties in growing and handling the material²; we suggest that this also results from the "s shift" (i.e., selectivity increasing the bonding energy of the Hg valence s levels, which weakens the Hg-Te bond and leads to the difficulties mentioned above).

It is our hope that this paper will stimulate work to test our suggestions. Such work is greatly needed, both for fundamental understanding and to guide (and reduce the cost of) practical work.

This work was supported by U. S. Defense Advanced Research Projects Agency Contract No. MDA 903-80-C496 and U. S. Air Force Office of Scientific Research Contract No. F49620-81-K0012; work was performed at the Stanford

Synchrotron Radiation Laboratory, which is supported by the National Science Foundation in cooperation with the U. S. Department of Defense. One of us (J.A.S.) was the recipient of a National Science Foundation predoctoral fellowship.

^(a)Permanent address: Fysisk Institut, Odense University, Capusvej 55, DK-5230, Odense M, Denmark.

¹See, for example, *Band Structure Spectroscopy of Metal and Alloys*, edited by D. J. Fabian and L. M. Watson (Academic, London, 1973).

²See, for example, R. Dornhaus and G. Nimtz, in *Solid-State Physics*, Springer Tracts in Modern Physics Vol. 78 (Springer-Verlag, Berlin, 1976), p. 1 and references therein.

³P. Morgen, J. Silberman, I. Lindau, W. E. Spicer, and J. A. Wilson, *J. Cryst. Growth* **56**, 493 (1982); P. Pianetta, I. Lindau, C. M. Garner, and W. E. Spicer, *Phys. Rev. B* **18**, 2792 (1978); P. Pianetta, I. Lindau, P. E. Gregory, C. M. Garner, and W. E. Spicer, *Surf. Sci.* **72**, 298 (1978).

⁴J. A. Silberman, P. Morgen, I. Lindau, W. E. Spicer, and J. A. Wilson, to be published; W. E. Spicer, in *Optical Properties of Solids—New Developments*, edited by B. O. Seraphin (North-Holland, Amsterdam, 1976).

⁵A.-B. Chen and A. Sher, *Phys. Rev. B* **23**, 5360 (1981).

⁶D. J. Chadi, J. P. Walter, and M. L. Cohen, *Phys. Rev. B* **5**, 3058 (1972).

⁷A. O. E. Animalu, *Philos. Mag.* **13**, 53 (1966).

One-Dimensional Localization and Interaction Effects in Narrow (0.1- μm) Silicon Inversion Layers

W. J. Skocpol, L. D. Jackel, E. L. Hu, R. E. Howard, and L. A. Fetter

Bell Laboratories, Holmdel, New Jersey 07733

(Received 1 March 1982)

The conductance of narrow (0.1- μm) silicon inversion layers has been measured at low temperatures. A divergent, nonmetallic decrease of conductance is observed below 30 K, in excellent quantitative agreement with the combined theories of weak localization and interaction effects in their one-dimensional form, if one assumes parameters comparable to those observed in wide (two-dimensional) inversion layers. In this novel experimental system both localization and interaction effects are present and comparable in size.

PACS numbers: 71.55.Jv, 72.15.-v, 73.40.Qv

Narrow [quasi one-dimensional (1D)] metal wires become nonmetallic at low temperatures.¹ The decrease of conduction is proportional to

e^2/\hbar and appropriate electron diffusion lengths, according to theory,² whenever these lengths exceed the transverse wire dimensions (the

quasi-1D case). Quantitative comparisons with theory³ have been complicated by having to compare small temperature-dependent changes ($\ll 1\%$) in different samples of varying width and resistivity in different materials, often with poorly characterized materials parameters. Many of the observed effects seem due to interaction effects proportional to the diffusive interaction length $L_{int} = (D\hbar/2k_B T)^{1/2}$ where D is the diffusion constant and T is the temperature, and much uncertainty continues about the role of localization effects proportional to the inelastic diffusion length $L_{inel} = (D\tau_{inel})^{1/2}$. The inelastic scattering time τ_{inel} in particular is a relatively unknown material parameter. In contrast, much more is known about the relevant length and time scales in silicon inversion layers, in which the conductivity and diffusion constant of the electrons can be easily varied by changing the gate voltage on a single device.

Applying recent advances in microfabrication technology, we have made silicon-inversion-layer channels only 100 nm wide which satisfy the 1D criterion, and show nonmetallic changes with temperature representing large fractional effects. Thus we are able to provide a graphic overview of the phenomena in a novel experimental context which allows direct quantitative comparison with the theory. We conclude that the results are in good agreement with the combined localization and interaction predictions.

We have fabricated⁴ a number of metal-oxide-silicon field-effect transistors (MOSFETs) with channel widths between 100 and 150 nm and mobilities at 4 K of 1000–4000 $\text{cm}^2/\text{V sec}$. The mobilities and thresholds of the devices are improved by annealing (limited to 300 °C by the use of gold metallization) and are degraded by prolonged stress at high gate voltages. Fortunately, the experiment described here is insensitive to these parameters, so long as an adequate conduction level can be achieved. Narrow-channel devices were compared with wider channels fabricated at the same time. For consistency we will illustrate this Letter with data from a particular pair of devices, typical of the results obtained. One device has a wide rectangular gate 20 μm wide by 8 μm long (0.4 squares), the other a parallel array of fourteen narrow gates each 100 nm wide by 5 μm long (4 squares, including spreading at the ends). To confine the inversion layer beneath each gate we used the NiCr gate metallization (defined by electron beam lithography) as a self-aligning mask for reactive ion

etching of material not directly under the gate. Figure 1 shows the ends of several narrow channels. Each wide end region contacts two separate diffused n^+ regions, allowing four-terminal measurements of the conductance of the array, including end regions. The gate oxide was 100 nm thick and the total etched depth was about 300 nm, so that the inversion layer formed at the SiO_2/Si interface less than halfway down the etched pedestal. Our confinement scheme is effective both in the low-conductance, strongly localized regime studied in recent experiments on electrically confined narrow channels,⁵ and in the higher-conductance weakly localized regime studied here where metallic behavior would be expected were it not for the quantum corrections.

We measured the small-signal ac conductance at source-drain voltage $\langle V_{DS} \rangle = 0$, as a function of V_G and temperature, T . The ac amplitude ($< 100 \mu\text{V}$) was adjusted so that negligible self-heating of the device occurred. Figure 2 shows G_{\square} vs V_G for both the narrow and wide devices. Although the narrow channels have a higher threshold voltage at which conduction begins, the differential mobility dG_{\square}/dV_G is only somewhat smaller than in the wide device, suggesting that the width of the channel has not been underestimated.

An overview of the various regimes of nonmetallic behavior predicted by theory is obtained by examining the temperature dependence of the conductance. The wide (2D) device shows substantial

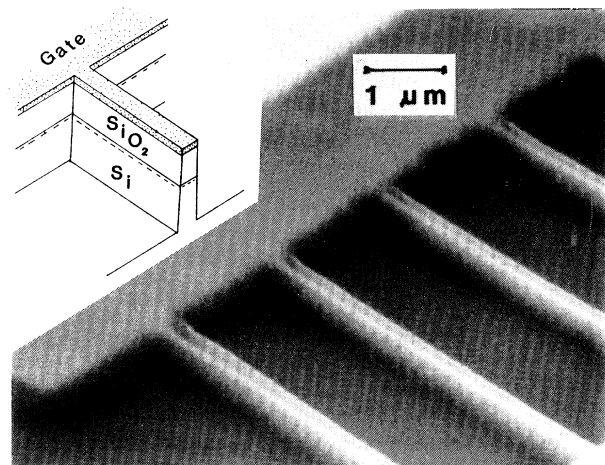


FIG. 1. A scanning electron micrograph, giving a perspective view of several of the narrow channels, approaching the wider end region. Reactive ion etching was used to confine the inversion layer at the Si/SiO_2 interface to the same width as the narrow metal gate.

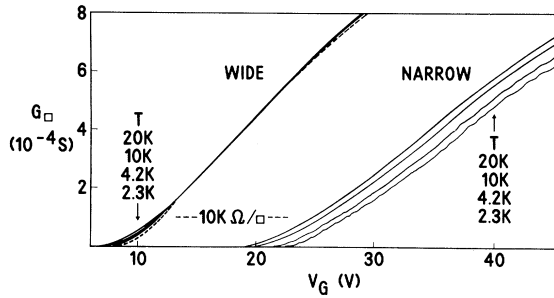


FIG. 2. A plot of G_{\square} vs V_g for both wide and narrow gate devices, at different values of T . The narrow device shows substantial nonmetallic changes with temperature, T .

temperature dependence only for $G_{\square}^{mm} \leq (10 \text{ k}\Omega/\square)^{-1} \approx e^2/\pi\hbar$, the “minimum metallic conductance” below which “strong localization” in the random impurity potential occurs. At higher conductance levels the nonmetallic 2D “weak localization” effect (only logarithmically divergent and ordinarily studied at much lower temperatures) is almost canceled at these temperatures by the metallic conductance changes ordinarily observed at higher temperatures. In contrast, the narrow (1D) device shows a much stronger nonmetallic variation of the conductance with temperature, exhibiting large fractional changes even up to $T = 20 \text{ K}$ and for G_{\square} exceeding $(1 \text{ k}\Omega/\square)^{-1}$, due to a combination of 1D “weak localization” and “interaction” effects.

The weak-localization and interaction effects can both be derived as quantum mechanical corrections to the conductivity within a microscopic perturbation theory that accounts for electron scattering by impurities and screened Coulomb interactions between the electrons.⁶ The localization correction results from electrons which interact repeatedly with impurities until their quasiparticle lifetime is limited by inelastic electron-electron scattering. The term describes coupling between states of nearly opposite momentum, which suggests backscattering into standing waves of weakly localized states, and hence a decrease of conductivity. The interaction correction results from electrons and holes of nearly equal momentum which interact repeatedly with impurities, thus affecting the many-body Coulomb interactions among the electrons. To first order the two terms simply add, and for a 1D channel of length L , predict² that

$$\Delta GL = (e^2/2\pi\hbar) (D\tau_{inel})^{1/2} + (4 - 2F)(D\hbar/2k_B T)^{1/2}. \quad (1)$$

Since $F \approx 1$ for well screened systems, the interaction effect does not approximately cancel here as it does in the 2D theory.

Quantitative comparison between theory and experiment requires values for the parameters D and τ_{inel} , which are well characterized in 2D inversion layers (ordinary MOSFETs), but are less certain in narrow channels. The 2D diffusion constant $D_2 = \frac{1}{2}v_F l$ together with the uniform 2D density of states $N_2 = 2m^*/\pi\hbar^2$ directly determine $G_{\square} = D_2 e^2 N_2$ in 2D inversion layers. In narrow channels the density of states N_1 may have substructure due to quantized transverse motion, but if averaged over width variations and other inhomogeneities, N_1 should average to the same N_2 per unit area. Thus we assume

$$D_1 = v_F l = 2G_{\square}/e^2 N_2 \quad (2)$$

as a reasonable approximation. The inelastic scattering time (predominantly electron-electron) has been measured in 2D inversion layers⁷ and agrees with recent theoretical calculations.⁸ We can summarize the results of Bishop, Dynes, and Tsui as yielding

$$\tau_{inel} = (2.5 \times 10^{-13} \text{ sec}^2 \text{ K/cm}^2) D/T. \quad (3)$$

The inelastic scattering time in narrow channels has been suggested to be longer with a weaker temperature dependence than in wide channels, but preliminary magnetoconductance measurements⁹ suggest that it may be shorter. In the absence of further information, we will compare our results with the 2D time given above. If the 2D proportionality of τ_{inel} to D/T still approximately holds, then the localization term in (1) has approximately the same $T^{-1/2}$ temperature dependence as the interaction term, but a stronger dependence on D , hence G_{\square} . Channels of various widths or mobilities which satisfy the 1D criterion should all show the same ΔGL when compared at equal G_{\square} .

Figure 3 plots G_{\square} vs T at fixed $V_G - V_T$ for the same devices as in Fig. 2, but following a 60°C “anneal” which apparently unloaded charged traps, increasing the mobility slightly, and decreasing the threshold voltages V_T to 5 and 10 V, respectively. When compared at equal G_{\square} , the temperature-dependent changes ΔG observed before and after “annealing” are approximately equal, demonstrating the universality predicted by the theory. Our other narrow samples, some annealed to $200\text{--}300^\circ \text{C}$, are in similar quantitative agreement.

In Fig. 3, the wide device shows a weak diver-

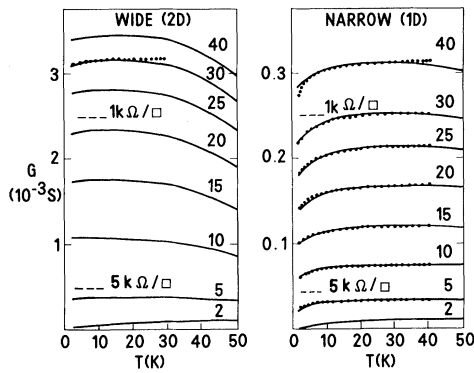


FIG. 3. A plot of G vs T for both wide and narrow gate devices after an overnight anneal at 60°C . The curves are labelled with $V_G - V_T(77\text{ K})$ in volts. The dotted curve on the left is the 2D theory, which is predicted to show the same change in conductance for each curve. The dotted curves on the right are the 1D theory, fitted with no adjustable parameters.

gent decrease at low temperatures in competition with an increasing metallic background. The dotted curve is ΔG_{\square} derived from 2D theory, under the assumption of constant background, and applies for all G_{\square} and any 2D width. The narrow device shows a much stronger divergence ΔG_{\square} when compared to the wide device at equal G_{\square} . The dotted curves for the 1D data are an empirical expression

$$\frac{\Delta GL}{e^2/2\pi\hbar} = (8.5 \times 10^{-6} \text{ cm K}^{1/2}) \times \frac{g^{1/2}}{T^{1/2}} [1.1g^{1/2} + 2], \quad (4)$$

which predicts the magnitude and temperature dependence of the conductance change at each gate voltage based on the measured high-temperature value of the conductance. Here $g = G_{\square}/(e^2/\hbar)$ is assumed proportional to D , and (4) is obtained by combining (1)–(3), with $m^* = 0.19m_0$ and $F = 1$. For the curves shown, g ranges from 0.6 to 5.2, so that the length scale in (4) exceeds the sample width and satisfies the 1D criterion at low temperatures. This formula gives an excellent fit to these data, and also to comparable data from the several other narrow ($< 150\text{-nm}$) devices, both annealed and unannealed, that we have investigated. In wider devices ($> 300\text{ nm}$), the effects are smaller and more 2D in character. Note here that both the temperature dependence and the variation of the magnitude of the changes with gate voltage are well accounted for. We have made no corrections for a metallic background term, since the data above 30 K suggest that the metallic background changes are dis-

tinctly smaller in the narrow channels. Even if the full metallic correction inferred from the discrepancy between 2D theory and experiment is included with the 1D theory, it results only in minor changes in the quality of fit below 20 K , where the divergent localization and interaction effects dominate. Since the localization and interaction terms are of similar magnitude, have different dependences on conductance g , and sum to approximately the correct magnitude, we are convinced that both are important. (In the range of conductances shown, the localization term increases from less than to more than the interaction term.) Despite the “no adjustable parameters” success of this fit, we remain aware that the observed scatter in the data, together with uncertainties in the parameters F , D , and τ_{inel} , means that this agreement is not a precision measurement of any particular parameter, such as τ_{inel} . Magnetoconductance measurements which isolate the localization term could more directly give values of $D\tau_{\text{inel}}$, for example, and such experiments will be of considerable interest.⁹

In conclusion, we have fabricated a novel MOSFET analog of narrow metal wires, and have demonstrated the simultaneous presence of localization and interaction effects in good agreement with one-dimensional theory using parameters estimated from two-dimensional results.

We have benefitted from useful discussions with R. G. Wheeler, D. E. Prober, R. C. Dynes, P. A. Lee, and S. K. Tewksbury. Our optical masks and electron-beam patterns were coded by R. H. Bosworth and R. W. Epworth. P. Grabbe and D. M. Tennant assisted in the device fabrication, which was done in part with use of furnaces of the Si Research Facility under the supervision of A. M. Voshchenkov.

¹N. Giordano, W. Gilson, and D. E. Prober, *Phys. Rev. Lett.* **43**, 725 (1979); see also subsequent investigations cited in A. E. White, M. Tinkham, W. J. Skocpol, and D. C. Flanders, *Phys. Rev. Lett.* **48**, 1752 (1982).

²D. J. Thouless, *Solid State Commun.* **34**, 683 (1980), and references therein; B. L. Altshuler, D. Khmel'nitzkii, A. I. Larkin, and P. A. Lee, *Phys. Rev. B* **22**, 5142 (1980).

³White, Tinkham, Skocpol, and Flanders, Ref. 1.

⁴W. J. Skocpol, A. M. Voschenkov, L. D. Jackel, R. E. Howard, E. L. Hu, R. W. Epworth, L. A. Fetter, P. Grabbe, and D. M. Tennant, to be published.

⁵A. B. Fowler, A. Hartstein, and R. A. Webb, *Phys. Rev. Lett.* **48**, 196 (1982).

⁶For a review of 2D theory, see H. Fukuyama, Surf. Sci. 13, 489 (1982).

⁷R. G. Wheeler, Phys. Rev. B 24, 4645 (1981); D. J. Bishop, R. C. Dynes, and D. C. Tsui, Phys. Rev. B 26,

773 (1982).

⁸E. Abrahams, P. W. Anderson, P. A. Lee, and T. V. Ramakrishnan, Phys. Rev. B 24, 6783 (1981).

⁹R. G. Wheeler, private communication.

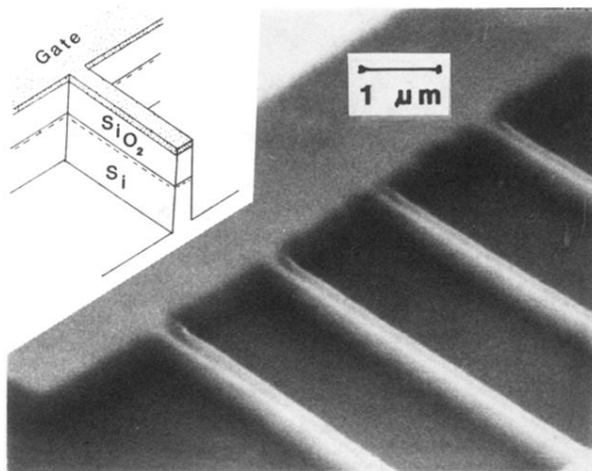


FIG. 1. A scanning electron micrograph, giving a perspective view of several of the narrow channels, approaching the wider end region. Reactive ion etching was used to confine the inversion layer at the Si/SiO₂ interface to the same width as the narrow metal gate.